Adaptation of the near-surface wind to the development of sand transport

By IAN K. McEWAN AND BRIAN B. WILLETTS

Department of Engineering, University of Aberdeen, Fraser Noble Building, Kings College, Aberdeen AB9 2UE, UK

A model of wind-blown sand transport is described with particular emphasis on the feedback between the grain cloud and the near-surface wind. The results from this model are used to develop Owen's (1964) hypothesis that 'the grain layer behaves, so far as the flow outside it is concerned, as increased aerodynamic roughness whose height is proportional to the thickness of the layer'. The hypothesis is developed to show the influence this dynamic roughness has on the turbulent boundary layer above the saltation layer. Two processes are identified which influence the path of the system towards equilibrium. The first is the feedback between the near-surface wind and the grain cloud in which the quantity of sand transported is limited by the carrying capacity of the wind. The second is due to the temporal development of an internal boundary layer in response to the additional roughness imposed on the flow above the grain layer by the grain cloud. A similarity is noted between the temporal response of a turbulent boundary layer to sand transport and the spatial response of a turbulent boundary layer downstream of a step increase in surface roughness. Finally it is noted that the work may have important implications for transport rate prediction in unsteady winds.

1. Introduction

Owen (1964) recognized that the drag imposed on the wind by the grain cloud during wind blown sand transportation acts as an increased roughness to the flow outside the grain layer. He argued that the new roughness length imposed on the flow was proportional to the height the grains travelled above the surface. Owen supposed that the vertical lift-off velocity was proportional to the shear velocity of the flow. Thus the effective roughness was given by

$$z_0' = C_0 U^{*'2}/2g,\qquad(1)$$

where z_0' is the effective roughness length, C_0 is an empirical constant, and $U^{*'}$ is the shear velocity during saltation.

Owen (1964) found, from the analysis of wind tunnel data, that for blown sand C_0 was roughly 0.02. Charnock (1955) arrived at a similar relationship for the roughness length for wind blowing over a water surface. In this case the argument was entirely from dimensional considerations whereas Owen's argument for blown sand has some physical basis. Charnock ascribed empirically from wind profile data a value of 0.013 to C_0. Wu (1969) reports from laboratory experiments a value of 0.0312 and Hicks (1972) in experiments over the Bass Strait and Lake Michigan found a mean value of 0.032. However Kitaigorodskii (1969) found published values ranging from 0.006 to 0.154.

Radok (1968) was, according to Tabler (1980), the first to apply Owen's roughness

relationship to blowing snow. Kind (1976) has demonstrated that wind profiles measured during transport of blown snow are in general agreement with Owen's relationship. Maeno *et al.* (1979) have also used the relationship to describe saltation in snow. Chamberlain (1983) drew attention to the similarity between the parameterization of the roughness length for snow, sand and sea.

Thus there is a feature common to the behaviour of the mobile surfaces of sand, sea and snow subjected to a strong wind. Each of these surfaces adapts itself to the flow by changing roughness; thus a dynamic equilibrium between the roughness length and the flow can be inferred. Some insight into the nature of this equilibrium may be found in the literature on flow downstream of a step change in surface roughness. In this paper we argue that the temporal response of a fully developed boundary layer to a sudden temporal change in roughness length is broadly similar to the streamwise response of a boundary layer downstream of a change in surface roughness during steady conditions. The case of a sudden temporal change in surface roughness is allied to the behaviour of a dynamic roughness such as blown sand. Anderson & Haff (1988, 1991) and McEwan & Willetts (1991) have shown from numerical experiments that the response time of the grain/wind system is of the order of 1 s from incipience to saturation: Butterfield (1991) has provided experimental confirmation of this result. Physically this response time is set by the rate of grain entrainment either directly by the fluid or through the impact of other grains. Thus the roughness length of a loose sand surface can increase significantly in a time of the order of 1 s. It will be shown in this paper that this temporal increase in surface roughness is rapid in comparison to the time required for boundary-layer adjustment, which suggests that the onset of particulate transport can be modelled as a sudden increase in surface roughness as far as the flow above the saltation layer is concerned.

Elliot (1958) introduced the notion of the internal boundary layer which develops downstream of a step change in surface roughness. Antonia & Luxton (1971) found, from wind tunnel investigation, that the growth of the internal boundary layer height was given by $\delta_i \propto x^{0.79}$ and noted the similarity between this and the growth rate of a turbulent boundary layer in a uniform free stream. They concluded that the structure of the flow outside the internal boundary layer did not seem to be influenced by the new surface roughness. Bradley (1968) conducted experiments measuring the change in shear stress after a step increase in surface roughness. He found that the shear stress increased sharply, overshooting its equilibrium value and decaying, initially rapidly, to its equilibrium at a distance downstream of the roughness change. Jensen (1978) made a theoretical analysis which produced a simple model giving good agreement with Bradley's results. The model confirmed the marked overshoot of equilibrium stress and the initially rapid decay toward equilibrium.

Jensen (1978) found the shear stress after the roughness change to be given by

$$\tau_x/\tau_- = [1 - m/\ln(H/z_+)]^2, \tag{2}$$

where τ_x is the shear stress at distance x downwind of the roughness change, τ_- is the shear stress upwind from the roughness change, $m = \ln(z_-/z_+)$, z_+ is the downwind roughness length, z_- is the upwind roughness length, and H is the boundary-layer height $[H/z_+ = (x/z_+)^{0.8}]$.

Figure 1 shows a plot of this relationship and data from Bradley (1968). A close match between theory and experiment is evident. However it should be noted that while Bradley's data indicate an equilibrium has been reached, equation (3) predicts a continued decay until at large x, $\tau_x \approx \tau$. However, as Jensen (1978) noted, x has to be very large indeed for this to occur. When $m = -2.3$ (a decade increase in roughness
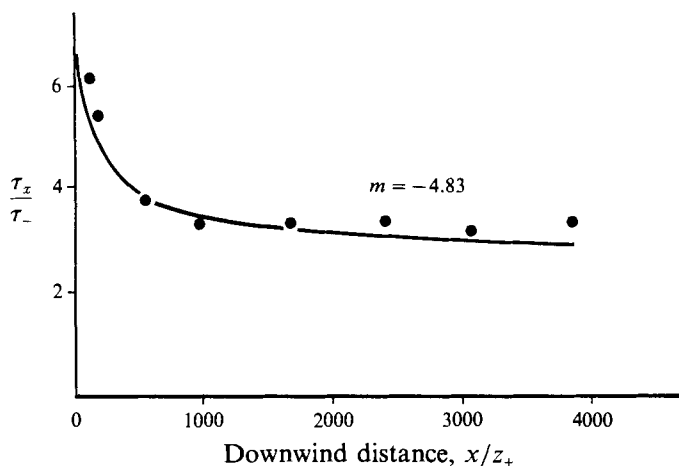
FIGURE 1. The variation of shear stress with distance downstream of a step change in surface roughness. Solid line: Jensen's (1978) model; circles: Bradley's (1968) data. The figure is taken from Jensen (1978). Note that Jensen (1978) argues strongly that the stress observed by Bradley cannot be the final equilibrium value.

length) and $z_+ = 0.001$ m, then at $x = 10$ m, τ_x is 15 % above its upwind value, at $x = 30$ m, τ_x is 13 % above its upwind value and at $x = 1000$ m, τ_x is still 10 % above its upwind value. Jensen's analysis shows that the progression toward boundary-layer equilibrium is slow and that a very considerable downstream length was required for the stress to approach its equilibrium value. On this basis Jensen indicated that the planetary boundary layer was unlikely to be in equilibrium except over some parts of the ocean where vast stretches of uniform roughness were available to the flow. It is noteworthy, in the context of this paper, that downstream of an increase in roughness an effective equilibrium at intermediate lengths is likely to be found in which conditions appear constant and the shear stress is greater than its equilibrium value.

Now consider Bagnold's account of the interaction between sand and the wind. Bagnold (1941) recognized that the grain cloud acted as an increased roughness to the flow. He observed that wind profiles measured during sand movement appeared to converge to a focus specified by a velocity (≈ 2.5 m/s) and a height (≈ 3 mm). He concluded that the wind profile was logarithmic above this height, emerging from the focal point. He introduced the symbol $U^{*\prime}$ to distinguish the shear velocity during sand transport from its clean-air counterpart. However, he also concluded that an increase in surface roughness caused the wind velocity to decrease by the same amount with height, thus the shear stress is independent of roughness (Bagnold 1941, p. 16). These two positions are not immediately reconcilable. This paper strongly supports the former one.

In this paper we will consider the influence of the sudden development of wind-blown sand transport on a neutral atmospheric boundary layer. A numerical model of wind-blown sand transport is described with particular emphasis on the algorithm used to model the feedback between the grain cloud and the wind. The results from this model confirm Owen's roughness hypothesis that the saltation layer acts as an increased roughness to the flow outside it and also support a postulated account of the effect on the boundary layer.
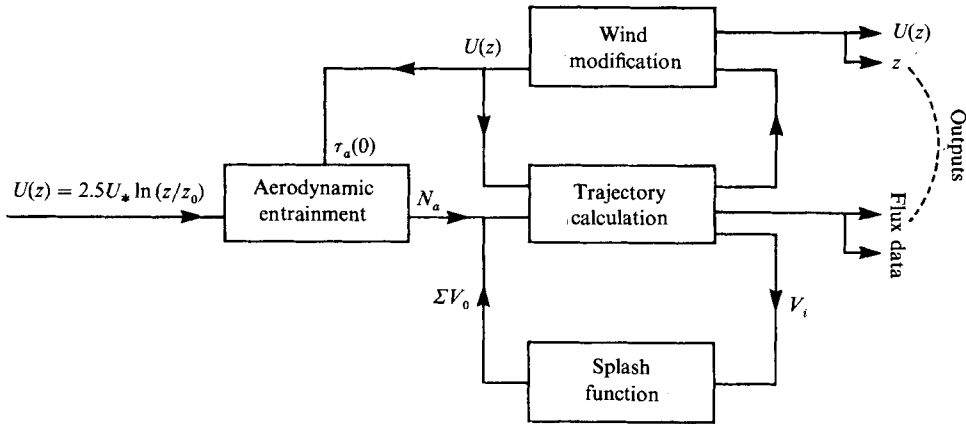
FIGURE 2. A schematic diagram of the linking of the four saltation subprocesses in the saltation model. The simulation begins with a clean-air logarithmic wind profile. Bed grains are entrained initially aerodynamically, then increasingly by the impact of saltating grains until their numbers are limited through a decelerating wind profile and the system reaches equilibrium.

2. Self-regulatory models of blown sand

Two self-regulatory models are known to exist which follow the development of sand transport from incipience through to steady state: Anderson & Haff (1988, 1991) and McEwan & Willetts (1991). The term 'self-regulatory model' refers to a built-in feedback mechanism which limits the steady-state transport rate. These models are constructed from the physics of the system, which is characterized as comprising four distinct subprocesses: aerodynamic entrainment, the trajectory of the grains, the grain/bed collision and the wind velocity modification (figure 2). Sand transport begins when the wind has sufficient traction on the surface to set some grains into motion. These grains roll or hop over the surface, gaining momentum, until they have sufficient energy on collision with the bed to cause the ejection of other bed grains into the flow. The grain population increases, principally because of the fertility of the grain/bed collision, until numbers are such that the grain cloud exerts a significant retarding force on the wind and the number of grains participating in saltation is thereby limited. The coupling of the four subprocesses which make up the wind-blown sand transport system is shown in figure 2.

The results presented in this paper are calculated by the self-regulatory saltation model of McEwan & Willetts (1991), and so an abbreviated description of the model will be given; fuller accounts are available in McEwan & Willetts (1991) and McEwan (1991). The emphasis in this paper is on the feedback between the grain cloud and the wind. The description of the model will, therefore, briefly touch on the first three sub-processes as defined above but give a fuller description of the fourth subprocess, the wind velocity modification. The reporting of model results will also follow this emphasis. It should be noted that, as reported in McEwan & Willetts (1991), the model compares well to available experimental evidence. In particular the expected nonlinear relationship between the sand transport rate and shear velocity is recovered as well as a roughly exponential decrease with height of the transport rate profile.

In the model of McEwan & Willetts (1991) aerodynamic entrainment is modelled by an excess shear stress law: the number of aerodynamically entrained grains is proportional to the difference between the fluid stress at the surface and the threshold shear stress for the sand. This is the same rule as that used by Anderson & Haff (1988, 1991). The grain trajectory model is well rehearsed in the literature. McEwan &

Willetts (1991) follow the precedent set by for example Anderson & Haff (1991), Hunt & Nalpanis (1985), White & Schulz (1977), Jensen & Sorensen (1986) and Ungar & Haff (1987). The grain/bed collision is modelled stochastically from data taken from high-speed films of the grain/bed collision for a natural quartz sand (Willetts & Rice 1985). Grains impact the surface at an acute angle (10°–16°) and ricochet at a steeper angle, typically in the range 20°–40° with a reduced speed of some 50–60% that of the incident grain. Several surface grains may be dislodged or ejected. These grains have an ejection speed of the order of 10% of the impact speed and have a broader distribution of lift-off angles, the mean being at 54° to the bed in the flow direction. A fuller description of the collision algorithm implemented in the self-regulatory model can be found in McEwan, Willetts & Rice (1993). In the calculation the grains are assumed to be spherical and of a uniform size.

3. The modification of the wind velocity profile

The general Navier–Stokes equation for fluid motion is simplified by assuming horizontally uniform flow and that $\partial/\partial z \gg \partial/\partial x$, $\partial/\partial y$. A body force acting in the streamwise direction is included which accounts for the effect of the grain motion. Thus we can write

$$\frac{\mathrm{d}U}{\mathrm{d}t} = \frac{\mathrm{d}}{\mathrm{d}z}\left[\nu\frac{\mathrm{d}U}{\mathrm{d}z}\right] + \frac{1}{\rho}F_x, \qquad (3)$$

where ν is the dynamic viscosity, F_x is a body force per unit volume exerted on the fluid in the streamwise direction by the grains, and ρ is the density of air.

Prandlt's mixing-length approximation is assumed to apply in which the eddy lengthscale is proportional to distance from the wall. While higher-order closure models are available their use here is not warranted and the simplest turbulent model was chosen.

Thus ν is specified by

$$\nu = \rho\kappa^2 z^2\,\mathrm{d}U/\mathrm{d}z \qquad (4)$$

and we have

$$\frac{\mathrm{d}U}{\mathrm{d}t} = \frac{\mathrm{d}}{\mathrm{d}z}\left[\rho\kappa^2 z^2\frac{\mathrm{d}U}{\mathrm{d}z}\frac{\mathrm{d}U}{\mathrm{d}z}\right] + \frac{1}{\rho}\sum_{i=1}^{n} m_i\left(\frac{\mathrm{d}v_x(z)}{\mathrm{d}t}\right)_i, \qquad (5)$$

where n is the number of grains per unit volume of fluid at height z, i enumerates each grain passing height z, (there is no distinction made between ascending and descending grains), m_i is the mass of grain i, $(\mathrm{d}v_x(z)/\mathrm{d}t)_i$ is the horizontal acceleration of grain i at height z, and κ is von Kármán's constant ($= 0.4$).

Thus the horizontal deceleration of the wind profile is assumed to consist of the balance of two forces. Firstly, a force is exerted on the wind by each entrained grain and, secondly, the fluid shear stress at z is modified by the change in velocity distribution arising from the grain activity. Only when these two streamwise forces balance is the wind steady ($\mathrm{d}U/\mathrm{d}t = 0$). The calculation begins by assuming an initially clean-air wind profile which is assumed to follow the law of the wall. The surface roughness length for this wind profile is specified by $\frac{1}{30}d$ where d is the diameter of the grains in the calculation (Nikuradse, as reported in Schlicting 1968).

The calculation space

The model domain is a space of nominal length and width and of infinite height. The grain trajectories are two-dimensional as lateral grain movement across the flow is precluded. The calculation space has a periodic boundary in the flow direction meaning

that a grain leaving the domain at one end immediately re-enters at the other with unchanged velocity. A significant penalty is attached to the use of a periodic boundary as it obscures the lengthscales of the saltation system, making impossible the calculation of such quantities as fetch (length taken for the grain cloud to reach equilibrium). Thus the mean quantities calculated by the model are assumed to be spatially homogeneous in the streamwise direction while wind velocity varies in the vertical direction. Thus the calculation follows the temporal evolution of the saltation system but cannot account for its streamwise development.

In the calculation the vertical dimension is discretized and during the simulation the wind profile is recalculated every 0.01 s (a typical trajectory duration is 0.1 s). The net force on each vertical discretization is calculated from equation (3) and is then used to determine the change in wind velocity at that height.

The local velocity gradient (dU/dz) is required to evaluate the first term on the right-hand side of (3); this is found from a numerical curve fitting on the mean wind profile. The grain trajectory calculation provides an account of the grain accelerations with height and in time and these are used to calculate the second term on the right-hand side of (3). This calculation is repeated for each time step throughout the simulation.

A boundary condition is required for the wind feedback calculation. The one chosen was to set the fluid shear stress well above the saltation layer equal to the sum of the grain borne and fluid shear stresses at the surface. This is the ultimate state of the saltation system when the boundary layer is in equilibrium but in nature it take a finite time for the fluid stress well above the saltation layer to reach the surface shear stress value. Thus it is a premature application of the boundary condition eventually attained by the physical system. The condition is time dependent because the total stress at the surface changes during the simulation. The consequences of using this boundary condition are discussed later.

The calculation method is similar to one used by Caldwell & Elliot (1972) to calculate the effect of rain on the surface wind. They also discretized the vertical dimension into slices and used the body force exerted by the falling rain drops to balance the differential shearing:

$$d\tau/dz = \text{body force.} \tag{6}$$

The analogy between rain and sand motion may be extended slightly further because Caldwell & Elliot (1972) noted that the rain imparts horizontal momentum to the surface on collision. This is similar to the grain/bed collision in sand which transfers momentum to the surface, leading to the evolution of bed topography.

4. A description of the model-generated saltation system

Perhaps the most important test of the self-regulatory model is to establish that it has reached an equilibrium, meaning that the wind and the saltation cloud have attained a time-averaged steady state. Figure 3 shows the transport rate variation during a 40 s period after the onset of saltation. The transport rate grows very rapidly during the first second until it reaches a maximum. Then it decays, initially rapidly, then more slowly, toward a presumed equilibrium which, for this simulation, is less than half its peak value. This decay to a steady state appears to take place over a time of the order of several tens of seconds.

Figure 4 and 5 show the response of the shear velocity and the effective roughness, respectively, over the same 40 s simulation period. The shear velocity was calculated from the gradient of the wind profile above 8 cm and the effective roughness was
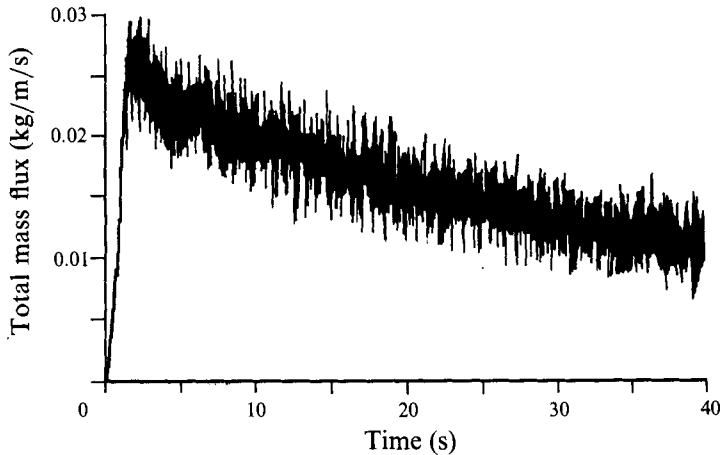
FIGURE 3. The total mass flux against time as calculated by the saltation model. The total mass flux was calculated at 0.01 s intervals. The initial shear velocity was 0.32 m/s; its development during the simulation is shown in figure 4.
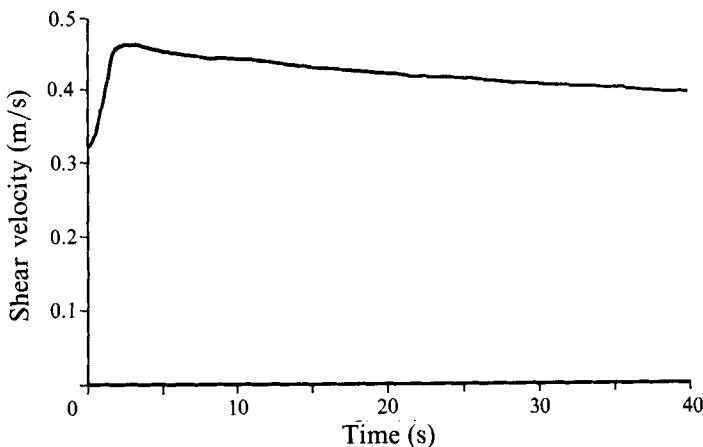
FIGURE 4. The shear velocity against time as calculated by the saltation model. The changes in shear velocity are roughly in phase with the development of total mass flux. The initial shear velocity was 0.32 m/s and the equilibrium value is approaching 0.4 m/s.

calculated from projecting an intercept of this gradient down to the height where the wind velocity would apparently be zero. The shear velocity, initially 0.32 m/s, rises rapidly in the first second. This rise is in phase with the initial increase in transport rate. Then the shear velocity and the roughness decay from their maximum values to a presumed equilibrium attained after several tens of seconds. Again this is in phase with the development of the transport rate in time.

It is noted that the behaviour of the system in time is similar to the spatial response of a boundary layer to a step change in roughness, shown in figure 1. In both cases the shear stress increases, overshooting its equilibrium value, and decays, initially rapidly, toward an eventual equilibrium.

The large difference between the maximum transport rate and the eventual equilibrium value occurs because of the highly nonlinear relationship between transport rate and the shear velocity.
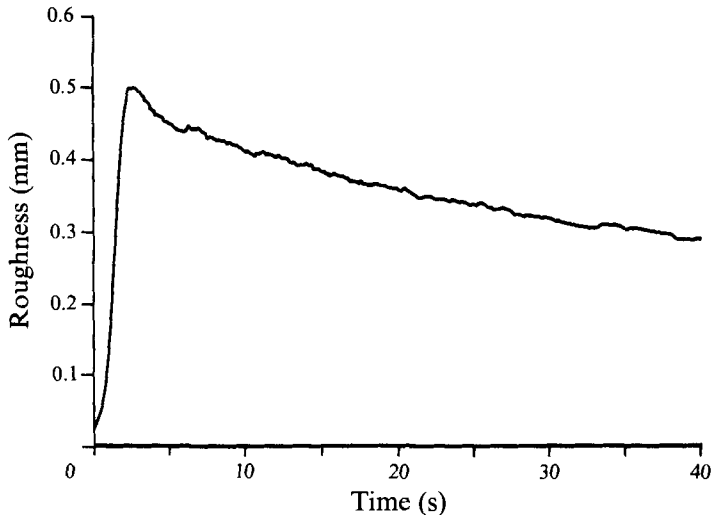
FIGURE 5. The effective roughness against time as calculated by the saltation model.

Thus the equilibrium of the saltation system can be considered as a two-stage process. Firstly, the saltating cloud responds rapidly (in less than one second) to a change in shear velocity. Secondly, the boundary layer must adjust to the increased roughness imposed on it by the saltation cloud. It does this by increasing its gradient (or shear stress). However this new shear stress is not in equilibrium with the upper boundary layer (or outer flow condition) and so a second equilibrium must be sought. This is done by a decrease in the shear stress over a period of the order of several tens of seconds. The first component of the steady state can be considered as the wind and the saltation cloud reaching an equilibrium and the second component as the new surface roughness and the wind profile moving toward equilibrium. It is only when roughly steady conditions have been attained over a much longer period relative to the first condition that the saltation system might be considered to be in equilibrium. However the use of the terms 'equilibrium' or 'steady state' in this context require qualification. Jensen's (1978) analysis of the planetary boundary layer indicates that vast lengths are required to attain an equilibrium boundary layer. Similarly the simulation described here has not yet attained an equilibrium or steady state but is reaching an effective equilibrium in which the rate of change in the boundary layer is small in comparison to the duration of the simulation; thus conditions are in effective equilibrium.

Figure 6 shows transport rate plotted against time for four shear velocities. The curves show the response time to reach the initial equilibrium decreasing with increasing shear velocity, in agreement with Anderson & Haff (1991). This arises because lower mean impact velocities are generated at lower U^*, causing fewer ejections. Thus the system takes longer to evolve to a steady state. Furthermore the 1 s response time of the system may be an overestimate during gusty winds as an already airborne saltation cloud will be 'instantaneously' accelerated by a gust rather than being developed from zero flux.

Figure 6 shows that the overshoot of the steady state decreases with decreasing U^*. This is to be expected as the increase in surface roughness is less at lower shear velocities, so the adjustment required from the boundary layer is not as great.

Attention has been drawn to the similarity of the response of the simulated wind profile in time to the streamwise response to a change in roughness. It is noted here that
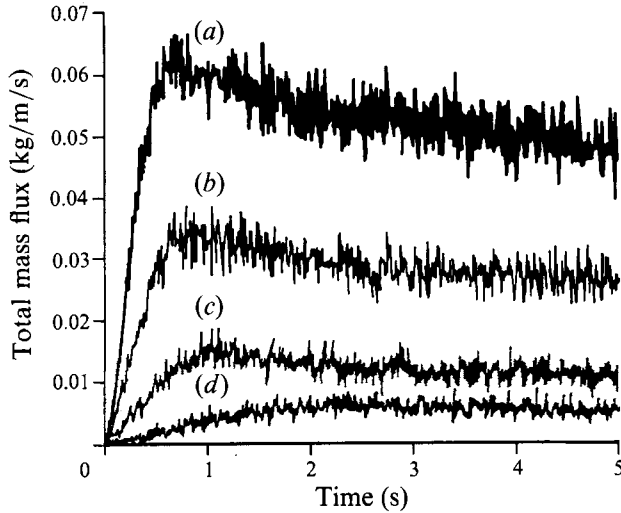
FIGURE 6. The total mass flux against time for four different shear velocities. (*a*) $U^* = 0.31$ m/s, (*b*) $U^* = 0.36$ m/s, (*c*) $U^* = 0.54$ m/s, (*d*) $U^* = 0.45$ m/s. As noted by Anderson & Haff (1991) the response time of the grain cloud appears to be a weak function of shear velocity.
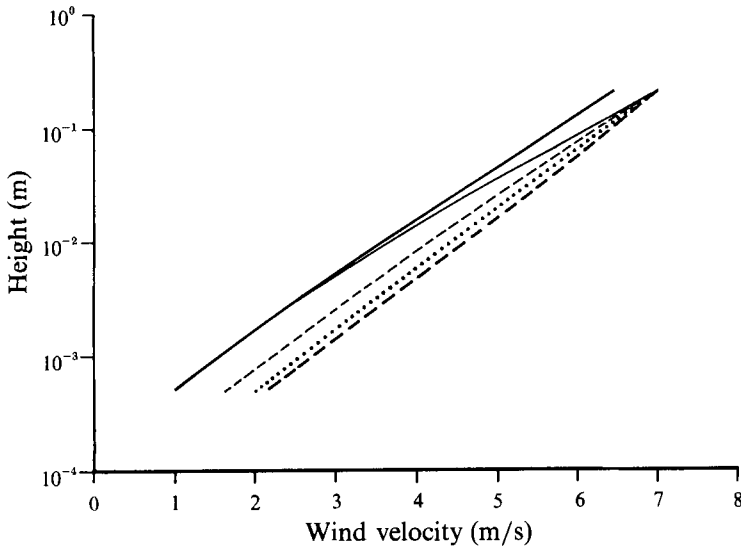
FIGURE 7. Wind profiles calculated by the model at $t = 0$ s (———), $t = 0.5$ s ($\cdots\cdots$), $t = 1.0$ s (— — —), $t = 2.0$ s (———) and $t = 40$ s (———). The initial shear velocity was 0.32 m/s; its development during the simulation is shown in figure 4. Note that the wind profile at $t = 2$ s meets the initial logarithmic wind profile at roughly $z = 0.12$ m. This corresponds to the height of the IBL at this time.

the development of the total mass flux in time (figure 6) and with distance appear to show a parallel development. Al-Sudairawa (1992) has shown that the fetch (length) required to attain an equilibrium saltation cloud increases with decreasing shear velocity. It is suggested that this is a similar effect to that shown in time in figure 6.

4.1. *The wind profile*

Figure 7 shows the wind profile calculated at $t = 0, 0.5, 1, 2$ and 40 s. The wind profiles at $t = 0.5$ and 1 s show the wind being decelerated toward the initial steady state by the grains. The wind at $t = 2$ s has the steepest gradient, indicating the maximum shear
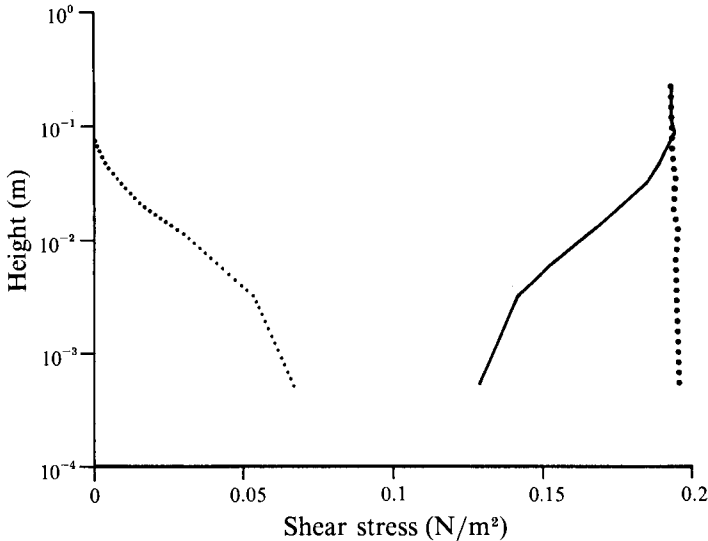
FIGURE 8. The fluid (Reynolds) stress (———), grain-borne shear stress (······) and the total shear stress (······) at $t = 40$ s. Note the complementary nature of the fluid and grain-borne stresses as the system approaches its steady state.

velocity. The wind profile at $t = 40$ s is similar to that at $t = 2$ s near the bed but has a smaller gradient at greater heights, indicating a reduction in shear stress.

During the growth of an internal boundary layer (IBL) the wind profile can reasonably be approximated by two logarithmic wind profiles, their intersection defining the height of the IBL or the boundary between modified and unmodified flow. Similar behaviour can be inferred from the wind profiles shown in figure 7. The initial clean-air logarithmic wind profile is shown by a long-dashed line. The wind profile at $t = 2$ s intersects the initial wind profile at roughly $z = 0.12$ m, and this height corresponds to the IBL height at $t = 2$ s. At $t = 40$ s the height of the IBL is obtained by extrapolating the wind profiles at $t = 0$ and 40 s to the height where they intersect. This is found to be roughly 10 m. This argument is qualitative only but it does represent an important step in the understanding of the wind modification in blown sand. Note that it would be incorrect to involve the wind profiles at $t = 0.5$ and 1 s in this argument because it is during this initial period that the grain cloud and hence the additional roughness is being established. The calculation is performed in the time domain, making the assumption of spatial homogeneity.

Figure 8 shows the airborne (Reynolds) stress, grain-borne shear stress and total shear stress (the sum of the airborne and grain-borne stresses) at $t = 40$ s. The airborne shear stress, found from equation (4), increases with height from a minimum at the surface to a maximum and constant value above the saltation layer. The grain-borne shear stress decreases from a maximum at the surface to zero above the saltation layer. The total stress, as predicted by Owen (1964) and assumed by Anderson & Haff (1988, 1991) is constant with height.

It is important to note that the two components of the shear stress in the saltation layer are calculated independently. The airborne shear stress is calculated from the local velocity gradient (dU/dz) and the eddy viscosity specified in equation (4), whereas the grain-borne shear stress is calculated by using the grain trajectory calculation to record the grains' change in forward velocity above a certain height. It
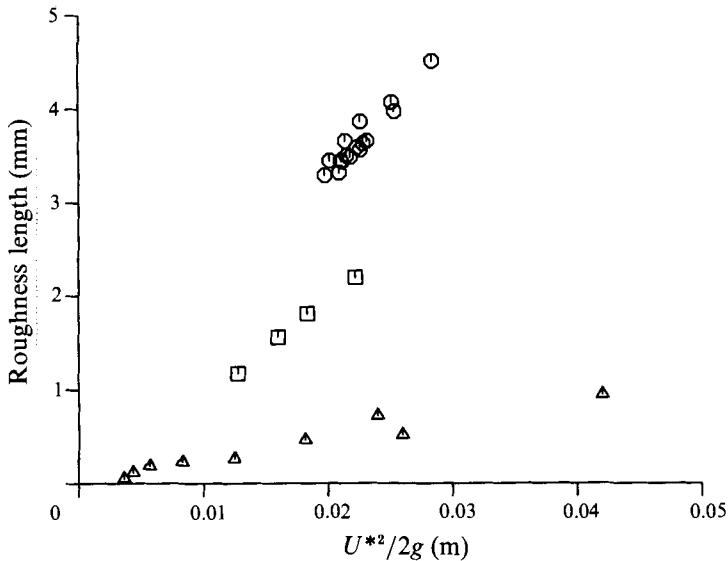
FIGURE 9. The effective roughness against $U^{*2}/2g$, as calculated by the numerical model ($\square$) and observed in a field experiment by Rasmussen *et al.* (1985) ($\odot$) and in the wind tunnel by Rasmussen & Mikkelsen (1991) ($\triangle$). The numerical model is in agreement that with Owen's (1964) suggestion that the additional roughness imposed on the flow by the grain cloud is proportional to $U^{*2}/2g$. It is noteworthy that results from the numerical model correspond more closely with the field data.

is a confirmation of the internal consistency of the model that the airborne and grain-borne stresses sum to give a constant total stress with height.

Figure 8 shows that there has been an increase in the shear stress due to saltation: the initial logarithmic shear stress is 0.13 N/m² whereas the total shear stress as the system nears an effective steady state has increased to 0.19 N/m².

4.2. *Roughness length*

Figure 9 shows three roughness data sets plotted against $U^{*2}/2g$ (see (1)). The first data set is from the Aarhus wind tunnel (Rasmussen & Mikkelsen 1991) and is consistent with $C_0 = 0.02$, the second data set consists of values calculated by the saltation model and is consistent with $C_0 = 0.11$ and the third set is data recorded by Rasmussen, Sorensen & Willetts (1985) in a field experiment conducted on a Jutland beach and is consistent with $C_0 = 0.18$. Anderson & Haff (1991) suggested that the discrepancy between field and wind tunnel results may be caused by the limited fetch available in a boundary-layer wind tunnel which denies the flow sufficient length to adjust completely to the new roughness.

Figure 10 and 11 show the mean impact velocity and the mean number of ejections respectively plotted against time. These plots suggest that an ingredient in the attainment of the steady state is the reduction in the mean impact velocity and the corresponding reduction in the mean number of ejecta per collision through time, as the wind is being decelerated. This feature of the saltation cloud explains the difference between the overshoot of the steady-state transport rate reported here and that found by Anderson & Haff (1988). Their overshoot is considerably smaller than the overshoot predicted by this saltation model, shown in figure 3. The reason for this is that the causes are different. The overshoot shown by Anderson & Haff (1988) is caused by a lag in the response of the saltation cloud to the rapid deceleration of the wind. In that model grains striking the surface at the time of the transport rate maximum have
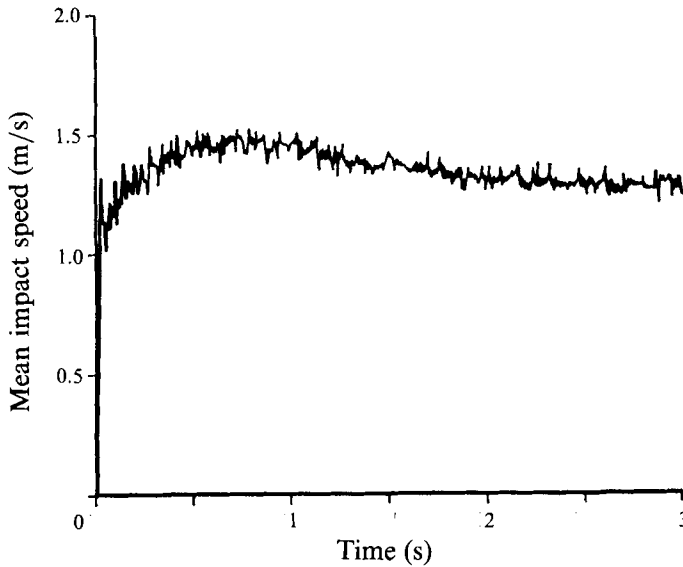
FIGURE 10. The variation of mean impact speed with time as calculated by
the saltation model at $U^* = 0.38$ m/s.
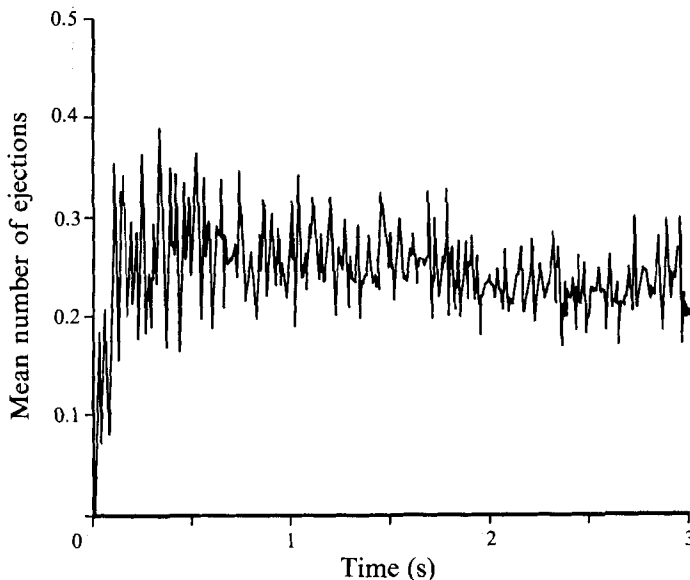
FIGURE 11. The relationship between the number of ejected grains and time
as calculated by the saltation model.

experienced higher wind velocities than the steady-state wind as they have travelled
through a decelerating wind profile. Therefore they impact the surface with impact
velocities higher than the eventual mean steady-state velocity. This feature of the
saltation cloud is also present in the model described here as evidenced in figure 10.
However, the much larger overshoot seen in figure 3 is dominated by the adjustment
of the boundary layer to a roughness change, a feature not accounted for in Anderson
& Haff (1988).
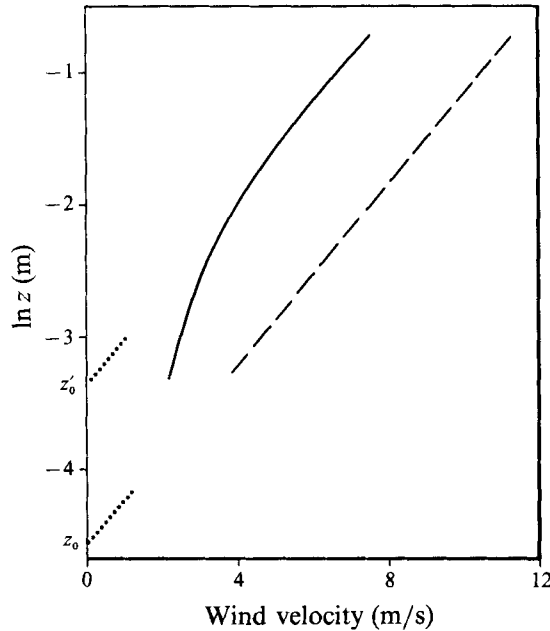
FIGURE 12. The wind velocity profile calculated by Anderson & Haff (1988). The dashed line is the initial wind profile and the solid line is the steady-state wind profile. Note the increase in the effective roughness of the surface and that the two wind profiles are parallel above the saltation layer, indicating no change in the shear velocity due to the increased roughness.

The wind velocity profile calculated by Anderson & Haff (1988) is shown in figure 12. The clean-air logarithmic wind profile is also shown. It is evident that the slopes of the two profiles are similar above the saltation layer, suggesting that the total stress is unchanged by the increased saltation roughness. Consideration of Anderson & Haff's calculation method shows why this is the case. They assume that the total shear stress is equal to the initial shear stress (before saltation) and is constant in time and with height throughout the calculation. However this cannot be the case. The increase in surface roughness due to saltation means that the total stress is not constant in time but should increase to a new constant value set by the far-field wind velocity and the effective roughness due to saltation. Constraining the shear velocity to its initial value results in the far-field velocity profiles being parallel before and after saltation on a logarithmic height scale and prevents the proper development of a fully modified boundary layer.

Anderson & Haff (1991) note this problem but conclude that it has a minor influence. However, results presented in this paper suggest that this is not the case. There is a substantial increase in the value of the total shear stress attributable to the increased roughness caused by the saltation cloud. Moreover there must be some question about the equilibrium state attained by the saltation model of Anderson & Haff (1988, 1991) because the increased roughness length calculated by their model, figure 12, cannot be in equilibrium with the imposed shear velocity, which is assumed to be constant throughout their calculation. This casts some doubt on whether that model's prediction of the nature of the relationship between the transport rate and shear velocity is correct. Rasmussen & Mikkelsen (1988) have indicated that some of the inconsistencies between transport rate prediction formulae stem from incomplete development of the wind tunnel boundary layer (for instance Kawamura 1951). They

I. K. McEwan and B. B. Willetts
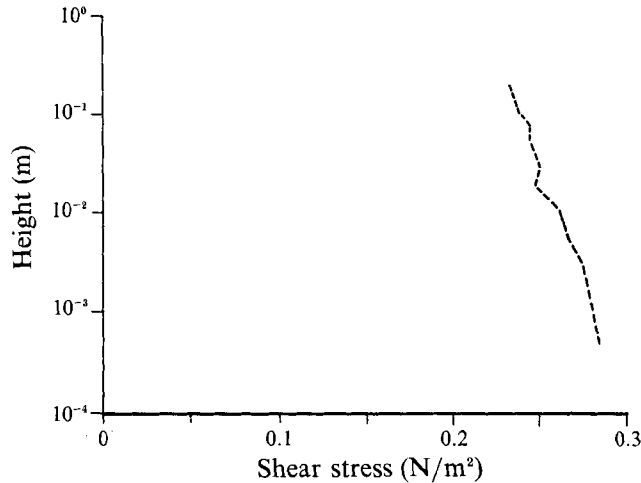
FIGURE 13. The total shear stress profile at $t = 1$ s after the onset of saltation
as calculated by the saltation model.

recommend that Owen's roughness relationship should be used as a check to ensure
that the effective roughness length and the shear velocity are consistent. This check
should also be applied to self-regulatory saltation models.

The difference between the shear velocities before and during saltation should be
noted. Bagnold (1941) introduced the symbol $U^{*\prime}$ to indicate the shear velocity in a
modified flow; unfortunately this precedent has not always been followed by
subsequent researchers and some confusion remains. The results from the self-
regulatory saltation model indicate clearly that U^* and $U^{*\prime}$ have different values and
must not be equated.

The self-regulatory saltation models of Werner (1990) and Sorensen (1991) are
steady-state models in that they do not calculate saltation from incipience through to
equilibrium in real time. Thus these two steady-state saltation models are able to
correctly assume a fully developed boundary layer and may calculate sand transport
in equilibrium with the wind velocity profile and the effective surface roughness.

5. The boundary condition in the self-regulatory model

The boundary condition in the reported saltation model sets the shear stress at a
height well above the saltation layer to be equal to the total shear stress at the surface.
This boundary condition is strictly appropriate only in the ultimate state of the system.
In nature the response of the boundary layer to the onset of saltation will propagate
upwards in time; this propagation is characterized by a rate of order U^*. Thus during
the period in which the saltation system is moving toward equilibrium the stress at the
surface will be greater than the stress well above the saltation layer. Therefore this
boundary condition is a premature application of the ultimately correct condition. In
the model, therefore, the stresses above and below the saltation layer are set to be the
same. It could be argued that this makes the steady state inevitable and possibly false,
but consideration of the fluid stress profile in figure 13 shows this not to be the case.
This figure shows the total stress profile (sum of grain-borne and airborne stresses)
calculated by the model at $t = 1$ s. The initial (constant) shear stress was 0.13 N/m² so
(at this time) the surface stress was 2–3 times its initial value. Consideration of this
profile shows there is no evidence of any distortion to the stress profile near the top of

the calculation space. If such a distortion were present it would take the form of an artificial increase in the stress near the top of the saltation layer resulting in a mis-shapen stress profile. Comparison of the stress profiles shown in figure 13 at $t = 1$ s and figure 8 at $t = 40$ s shows that the 'trajectory' of the stress profile through time is normal, being influenced by the surface from 'the bottom up'. Thus the boundary layer is developing correctly, almost uninfluenced by the use of a premature boundary condition.

6. Some concluding remarks

The wind calculation scheme used in this saltation model has led to further insight into the temporal scaling of the saltation cloud. Anderson & Haff (1988) estimated that the time required for the grain cloud to reach equilibrium with the wind is roughly 1 s. This has since been confirmed experimentally by Butterfield (1991). However a further significant temporal response has emerged from this study which shows that after an equilibrium grain cloud has been established a second, longer, adjustment is takes place as the flow comes into equilibrium with the additional roughness imposed by the grain cloud. The time required to approach this second effective velocity is of the order of several tens of seconds.

A useful interpretation of the system is found by regarding the first equilibrium as a sudden increase in surface roughness. If this approach is taken the temporal response of the boundary layer after the initial equilibrium is very similar to the spatial response of a boundary layer downstream of an increase in surface roughness. However some caution should be exercised that this analogy is not taken too far as it can mask an important property of the system. The effective roughness due to the grain cloud should be considered as a *dynamic roughness*, one that is able to respond to changes in the flow. Thus as the shear stress is moving toward equilibrium after over shooting its equilibrium value the sand transport rate decays in response to the reduction in the shear stress. Moreover because the roughness length is set by the grain cloud, it decreases approximately in phase with the shear stress and the sand transport rate. Thus there exists a dynamic equilibrium between the flow and the roughness length.

This work raises questions about what exactly constitutes steady-state sand transport. It appears that an effective equilibrium between the grain cloud and the boundary layer will not be approached until a relatively long period (several tens of seconds) has elapsed after any change. Furthermore the observation of Jensen (1978) that an equilibrium boundary layer is only attained over vast fetches of uniform roughness indicates that this second equilibrium is also transitory over much longer timescales. Thus it would appear, in the context of wind erosion in the atmospheric boundary layer, that equilibrium between flow and roughness is unlikely to be achieved either spatially or temporally. Thus measurements of sand transport rate in a gusty wind are not records of equilibrium transport but rather are the average of a sequence of adjusting flows. The notion of a dynamic roughness interacting with a developing boundary layer promises to be a useful concept in interpretating sand transport in unsteady winds and may represent some refinement of the accepted model of wind-blown sand transport.

REFERENCES

AL-SUDAIRAWI, M. 1992 The effect of non-erodible elements on sand transport rate. PhD thesis, University of Aberdeen.

ANDERSON, R. S. & HAFF, P. K. 1988 Simulation of aeolian saltation. *Science* **241**, 820–823.

ANDERSON, R. S. & HAFF, P. K. 1991 Wind modification and bed response during saltation of sand in air. *Acta Mechanica, Suppl.* **1**, 21–52.

ANTONIA, R. A. & LUXTON, R. E. 1971 The response of a turbulent boundary layer to a step change in surface roughness. Part 1. Smooth to rough. *J. Fluid Mech.* **48**, 721–761.

BAGNOLD, R. A. 1941 *The Physics of Blown Sand and Desert Dunes.* Methuen.

BRADLEY, E. F. 1968 A micrometeorological study of velocity profiles and surface drag in the region modified by a change in surface roughness. *Q. J. R. Met. Soc.* **94**, 361–379.

BUTTERFIELD, G. R. 1991 Grain transport rates in steady and unsteady turbulent airflows. *Acta Mechanica, Suppl.* **1**, 97–122.

CALDWELL, D. R. & ELLIOT, W. P. 1972 The effect of rainfall on the wind in the surface layer. *Boundary-Layer Met.* **3**, 146–151.

CHAMBERLAIN, A. C. 1983 Roughness length of sea, sand and snow. *Boundary-Layer Met.* **25**, 405–409.

CHARNOCK, H. 1955 Wind stress on a water surface. *Q. J. R. Met. Soc.* **81**, 639–640.

ELLIOT, W. P. 1958 The growth of the atmospheric internal boundary layer. *Trans. Am. Geophys. Union* **39**, 1048–1054.

HICKS, B. B. 1972 Some evaluation of drag and bulk transfer coefficients over water bodies of different sizes. *Boundary-Layer Met.* **3**, 201–213.

HUNT, J. C. R. & NALPANIS, P. 1985 Saltating and suspended particles over flat and sloping surfaces. In *Proc. Intl Workshop on Physics of Blown Sand, Memoirs 8, Dept. of Theoretical Statistics, Aarhus University, Denmark*, pp. 37–66.

JENSEN, J. L. & SORENSEN, M. 1986 Estimation of some aeolian saltation transport parameters: A re-analysis of Williams' data. *Sedimentol.* **33**, 547–558.

JENSEN, N. O. 1978 Change of surface roughness and the planetary boundary layer. *J. R. Met. Soc.* **104**, 351–356.

KAWAMURA, R. 1951 Study of sand movement. *Rep. Inst. Sci. Tech. Univ. Tokyo, vol. 5, pp. 1–2 (In Japanese).* (Available in English as *NASA Tech. Trans.* F-14, 215pp.)

KIND, R. J. 1976 A critical examination of the requirements for model simulation of wind induced erosion/deposition phenomena such as drifting snow. *Atmos. Environ.* **10**, 219–227.

KITAIGORODSKII, S. A. 1969 Small scale atmosphere-ocean interactions. *Izv. Atmos. Ocean Phys.* **5**, 1114–1131.

MCEWAN, I. K. 1991 The physics of sand transport by wind. PhD thesis, University of Aberdeen.

MCEWAN, I. K. & WILLETTS, B. B. 1991 Numerical model of the saltation cloud. *Acta Mechanica, Suppl.* **1**, 53–66.

MCEWAN, I. K., WILLETTS, B. B. & RICE, M. A. 1993 The grain/bed collision in sand transport by wind. *Sedimentology* **39**, 971–981.

MAENO, N., ARAOKA, K., NISHIMURA, K. & KANEDA, Y. 1979 Physical aspects of the wind–snow interaction in blowing snow. *J. Faculty of Sci. Hokkiado Univ.* VII (*Geophys.*) **6**, No. 1.

OWEN, P. R. 1964 Saltation of uniform grains in air. *J. Fluid Mech.* **20**, 225–242.

RADOK, U. 1968 Deposition and erosion of snow by wind. *US Cold Regions Res. and Engng Lab. Res. Rep. 230.*

RASMUSSEN, K. R. & MIKKELSEN, H. E. 1988 Aeolian transport in a boundary layer wind tunnel. *Geoskrifter* 28. Geologisk Institut, Aarhus Universitet.

RASMUSSEN, K. R. & MIKKELSEN, H. E. 1991 Wind tunnel observations of aeolian transport rates. *Acta Mechanica, Suppl.* **1**, 135–144.

RASMUSSEN, K. R., SORENSEN, M. & WILLETTS, B. B. 1985 Measurement of saltation and wind strength on beaches. In *Proc. Intl Workshop on Physics of Blown Sand, Memoirs 8, Dept. of Theoretical Statistics, Aarhus University, Denmark, pp. 301–326.*

SCHLICTING, H. 1968 *Boundary Layer Theory*, 6th edn. McGraw-Hill.

SORENSEN, M. 1991 An analytic model of wind-blown sand transport. *Acta Mechanica, Suppl.* 1, 67–82.

TABLER, R. D. 1980 Self-similarity of wind profiles in blowing snow allows outdoor modelling. *J Glaciol.* 26, 421–434.

UNGAR, J. E. & HAFF, P. K. 1987 Steady state saltation in air. *Sedimentol.* 34, 289–299.

WERNER, B. 1990 A steady state model of wind-blown sand transport. *J. Geol.* 98, 1–17.

WHITE, B. R. & SCHULZ, J. C. 1977 Magnus effect in saltation. *J. Fluid Mech.* 81, 497–512.

WILLETTS, B. B. & RICE, M. A. 1985 Inter-saltation collisions. In *Proc. Intl Workshop on Physics of Blown Sand, Memoirs 8, Dept. of Theoretical Statistics, Aarhus University, Denmark, pp. 83–100.*

WU, J. 1969 Wind stress and surface roughness at the air–sea interface. *J. Geophys. Res.* 74, 444–455.